CAV2021
11th International Symposium on Cavitation
May 10-13, 2021, Daejeon, Korea

Characteristics of a Hydrofoil Flutter under Cavitation Conditions

Tatsuya Irie [1]*, Shunsuke Nakai [1], Kazuyoshi Miyagawa [1], Chiharu Kawakita [2] and Koichiro Shiraishi [2]

[1]Department of Applied Mechanics and Aerospace Engineering, Waseda University, Japan
[2] National Maritime Research Institute, National Institute of Maritime, Port and Aviation Technology, Japan

Abstract: Marine propellers built of composite material may experience a flutter undesirable to the safe operation. However, the flutter instability of the flexible hydrofoil in a cavitating stream has yet to be elucidated. In this paper, we investigate the flutter on flat-plate hydrofoils installed in a cavitation tunnel. The foils have been tested with and without cavitation with an attack angle of eight degrees. In non-cavitating stream, the foils experience a coupled flutter. At this moment, the bending and the torsional strains are interacting reciprocally. It has turned out that the flutter-inception velocity can be assessed by the reduced frequency, regardless of the foil material. In cavitation conditions, including partial, transitional, and supercavitation, the flutter-inception velocity is shifted toward lower, higher, and higher by far, respectively. To conclude, the hydrofoil features different flutter behaviors in cavitation conditions.

Keywords: Composite Propeller, Cavitation, Hydrofoil, Flutter, Self-excitation

1. Introduction

Composite materials represented by CFRP or GFRP feature light mass and high pliability. They deform in response to the load imposed, therefore improving cavitation or hydraulic performance [1-2]. Hence, they have been adopted for ship propulsion in recent years [3]. However, an elastic blade generally experiences destructive self-exciting phenomena as the flutter instability. It has been dealt with as an important issue in aerodynamics [4]. For the case of hydrofoil, Peter [5] introduced the flutter speed evaluating the flutter inception. Matsudaira et al. [6] experimentally studied the flutter stability in the sub-cavitation region. Nonetheless, there is still open questions regarding the influence of the material and the cavitation patterns on the hydrofoil flutter instability. This paper investigates the flutter characteristics of a flat-plate hydrofoil with and without cavitation.

2. Materials and Methods

Figure 1(a) illustrates the top view of the cavitation tunnel. Figure 1(b) shows the dimension of the test section. Figure 1(c) and (d) give the testing piece drawings, where *C*, L.E., and T.E. are the chord length, the foil leading edge, and the trailing edge, respectively.

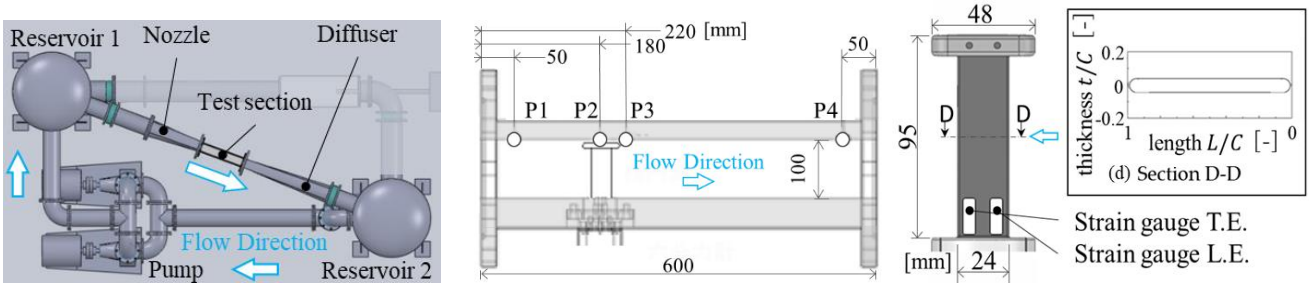

(a) (b) (c)

Figure 1. (a) The top view of the cavitation tunnel in Waseda Univ, (b) The side view of the test section, (c) The foil and the mass drawings, (d) The section view D-D. An arrow implies the flow direction.

* Corresponding Author: Tatsuya Irie, iritatsumarines1@toki.waseda.jp

We studied the flutter with distinct hydrofoil materials. Foils are mounted with A6061 mass on their tip to diminish their natural frequency f_n. The transient strain is measured by pairs of strain gauges adhered to the foil boss. The bending strain ϵ_b and the torsional strain ϵ_t are extracted from the Equation (1) and (2).

$$\epsilon_b = (\epsilon_{L.E.} + \epsilon_{T.E.})/2 \quad (1)$$

$$\epsilon_t = \epsilon_{L.E.} - \epsilon_{T.E.} \quad (2)$$

Table 1 shows the foil combination and the test condition.

Table 1. The foil combination and the test condition

Test condition	Value
Foil material	Acrylic, A6061, SUS304
Mass material	A6061
Maximum flow velocity	10 [m/s]
Test section dimension	100 × 100 [mm]
Blade attacking angle α	8 [deg]
Sampling frequency	8000 [Hz]

3. Results

3.1. Flutter test in no-cavitation conditions

Figure 2 and Figure 3 show the waterfall diagrams of the strain FFT amplitude in no-cavitation. The graphs are the results of the test piece combination SUS304 foil + A6061 mass. Via submerged hammering test, its natural frequencies f_n were measured as follows: bending-primary = 98.5 [Hz], bending-secondary = 670 [Hz], and torsion-primary = 584 [Hz].

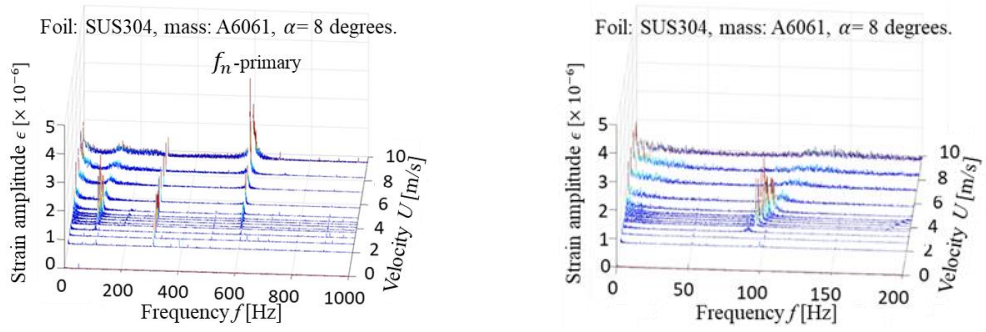

Figure 2. Waterfall diagrams of torsional strain. (a) Overall frequency, (b) Enlarged view.

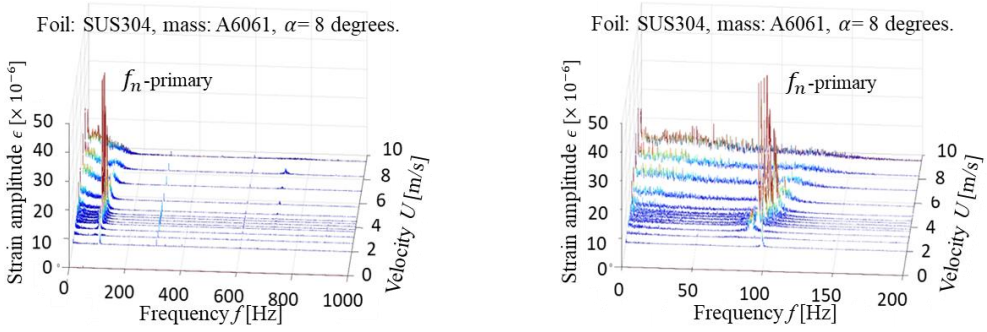

Figure 3. Waterfall diagrams of bending strain. (a) Overall frequency, (b) Enlarged view.

* Corresponding Author: Tatsuya Irie, iritatsumarines1@toki.waseda.jp

The frequencies independent of the velocity may be the natural frequencies of the hydrofoil. In Figure 2(b), a unique peak at a frequency different from $f_{\mathrm{n-torsion}}$ and dependent on the velocity is observed. This peak can also be observed in Figure 3 (b), and they feature a certain phase difference ϕ_i=79.0 [deg] at their first appearance. At this moment, the bending and the torsional motions are coupled, feeding back each other. We define this phenomenon as bending-torsion flutter, which will be mainly discussed in the following. In addition, at a small attacking angle, the forced vibration originated from a vortex shedding becomes dominant on the foil (not shown here).

Equation (3) defines the reduced frequency *K*. Table 2 lists the flutter inception results classified by the material combination. The inception can be judged comprehensively by introducing the *K*, regardless of the material. Among these choices, SUS304 foil + A6061 mass hydrofoil performed the most rigid structure. This foil produces all the cavitation patterns before it falls into the flutter.

$$K = \frac{\omega b}{U} \ [-] \ , \ \omega\text{: circular frequency [rad/s]}, \ b\text{: semi-chord length [m]} \tag{3}$$

Table 2. Flutter inception in different foil materials

Hydrofoil+Mass	**Acrylic+A6061**	**A6061+A6061**	**SUS304+A6061**
Flow velocity U_i [m/s]	0.77	2.7	3.8
Frequency f_i [Hz]	18.7	59.9	91.8
Phase difference between Bending/Torsion ϕ_i [deg]	70.3	77.0	79.0
Reduced frequency K_i [-]	1.8	1.7	1.8

3.2. SUS304 foil + A6061 mass hydrofoil flutter test in cavitation conditions

In this part, the influence of the cavitation pattern on the flutter characteristics is investigated. According to Brennen [7], the cavitation patterns can be classified into the following major criterion by scaling the cavity length: (a) Partial: unsteady cavitation, (b) Transient: coexisting state of steady partial cavitation and unsteady supercavitation, (c) Supercavitation. Figure 4 shows the cavitation patterns observed with different cavitation numbers given by Equation (4).

$$\sigma = \frac{2(P_1 - P_v)}{\rho U^2} \ [-], \ \rho\text{: density [kg/m}^3\text{]}, \ P_v\text{: saturated water vapor pressure [Pa]} \tag{4}$$

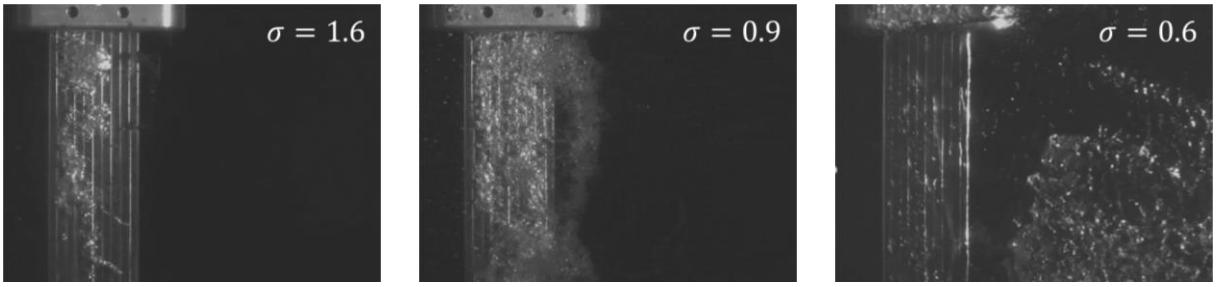

(a) (b) (c)

Figure 4. Cavitation patterns captured on the hydrofoil. Foil: SUS304, mass: A6061, $\boldsymbol{\alpha}$= 8 degrees. (a) Partial cavitation (cavity length *l*<3/4*C*), (b) Transitional cavitation (3/4*C*<*l*<4/3*C*), (c) Supercavitation (4/3*C*<*l*).

Table 3 shows the flutter inception results under different cavitation conditions. Figure 5 and Figure 6 show the waterfall diagrams of the FFT strain for each condition. In comparison to Figure 2, the incipient velocity U_i has decreased in partial cavitation flow, then promoting the flutter onset. In transient cavitation condition, the value of U_i increases. In super cavitation condition, the onset of the flutter is not observed within the tested range of velocity, from 0 [m/s] to 8 [m/s].

* Corresponding Author: Tatsuya Irie, iritatsumarines1@toki.waseda.jp

Table 3. Flutter inception under different cavitation conditions

Cavitation forms	(a) Partial	(b) Transitional	(c) Super
Cavitation number σ [-]	1.6	0.9	0.6
Flow velocity U_i [m/s]	3.59	4.24	-
Frequency f_i [Hz]	91.3	91.2	-
Phase difference between Bending/Torsion ϕ_i [deg]	124	102	-

Under the partial cavitation, the phase difference ϕ_i is 124 [deg] at U_i=3.59 [m/s], whereas, it is equal to 13 [deg] at the same velocity in non-cavitating flow. The cavity is concentrated on the L.E., and the partial cavitation itself behaves as an unsteady cavity [7]. This implies that the cavity at the L.E. affects the lift and drag characteristics of the foil and furthered the divergence of ϕ. Therefore, the feedback of bending-torsion is reinforced.

In transient and supercavitation conditions, the cavity is wrapping up the whole side of the foil. Thereby, the part of an added mass has been replaced by the cavity, resulting in an increase of the natural angular frequency ω_n. Equation (5) shows the definition of ω_n for this case. The suffix w and c indicate water and cavity, respectively.

$$\omega_n = \sqrt{\frac{k}{m+\Delta m_w-\Delta m_c}} \text{ [rad/s]}, \quad k\text{: spring constant [N/m]}, \ m\text{: mass [kg]}, \ \Delta m\text{: added mass [kg]} \tag{5}$$

Consequently, the flutter inception is shifted to a higher velocity. Furthermore, when the cavity is wrapping up the foil, the minimum pressure on the surface becomes no less than the vapor pressure. It reduces the external force on the blade, which is the trigger for the oscillation.

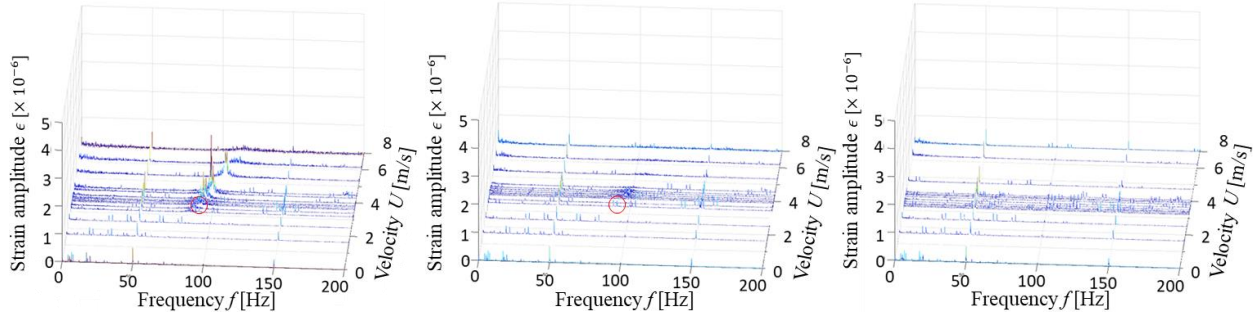

(a) (b) (c)

Figure 5. Waterfall diagrams of torsional strain. Foil: SUS304, mass: A6061, α= 8 degrees. (a) Partial cavitation (cavity length l<3/4C), (b) Transitional cavitation (3/4C<l<4/3C), (c) Supercavitation (4/3C<l).

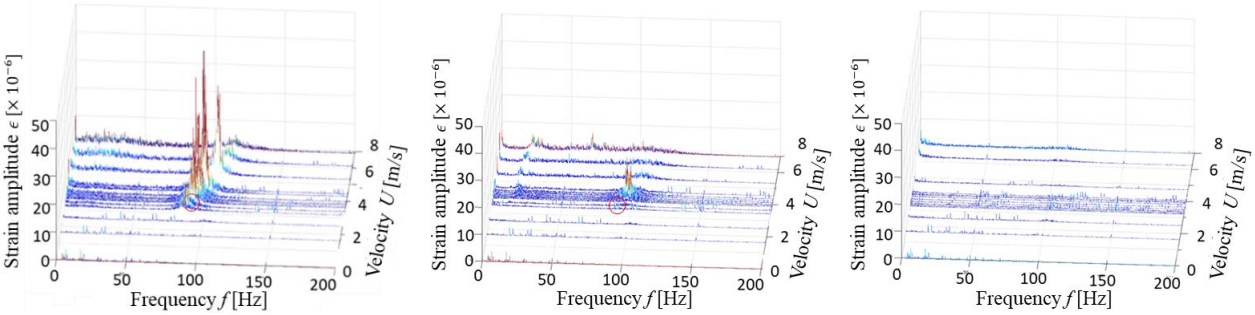

(a) (b) (c)

Figure 6. Waterfall diagrams of bending strain. Foil: SUS304, mass: A6061, α= 8 degrees. (a) Partial cavitation (cavity length l<3/4C), (b) Transitional cavitation (3/4C<l<4/3C), (c) Supercavitation (4/3C<l).

* Corresponding Author: Tatsuya Irie, iritatsumarines1@toki.waseda.jp

4. Conclusions

We investigated the coupled-hydrofoil flutter of bending-torsion in a cavitation tunnel. By using a reduced frequency, the flutter inception in non-cavitating flow can be evaluated, regardless of material. In cavitation conditions, the results showed that the cavitation pattern greatly influences the flutter inception. Due to its accelerated phase difference and the unsteady cavity, the flutter-incipient velocity decreases in partial cavitation conditions. In further developed cavitation conditions, the incipient velocity increases due to the mitigation of the external force and the increase of the natural angular frequency of the hydrofoil.

Acknowledgments: This research was supported by JSPS KAKENHI Grant Number JP18H01649. The authors would like to thank the Waseda Research Institute for Science and Engineering (WISE) for supporting the presented research, in the context of the project: 'High performance and high-reliability research for hydraulic turbomachinery systems'

References

1. S. Selvaraju and S. Ilayavel, Applications of composites in marine industry, *Journal of Engineering Studies and Research* **2011**, *2*, 89-91
2. M. R. Motley and Y. L. Young, Performance-based design and analysis of flexible composite propulsors, *Journal of Fluids and Structures* **2011**, *27*, 1310-1325
3. G. Marsh, A new start for marine propellers?, *Reinforced Plastics* **2004**, *48(11)*, 34-38
4. D.H. Hodges and G. A. Pierce, *Introduction to structural dynamics and aeroelasticity*, 2nd ed, Cambridge University Press, New York, The United States of America, 2011, pp.3-5, 75-202.
5. P.K. Besch and Y.N. Liu, Flutter and Divergence Characteristics of Four Low Mass Ratio Hydrofoils, Ship Performance Department Research and Development Report,1971
6. Y. Matsudaira and N. Okazaki, Fluid Force and Stability of a Pitching Hydrofoil in Subcavitation Region, *JSME International Journal Series B Fluids and Thermal E ngineering* **1998**, *41(3)*, 575-582
7. C.E. Brennen, *Cavitation and Bubble Dynamics*, Oxford University Press, New York, The United States of America, 1995, pp.270-272

* Corresponding Author: Tatsuya Irie, iritatsumarines1@toki.waseda.jp